AGU PUBLICATIONS

Geophysical Research Letters

RESEARCH LETTER
10.1002/2016GL072416

Key Points:
- Bidirectional estuarine exchange fluxes can be driven by coastal upwelling
- Ria de Vigo response to coastal upwelling is faster than the inertial period
- Remote wind with local wind and stratification modulate the rapid response

Correspondence to:
M. Gilcoto,
mgilcoto@iim.csic.es

Citation:
Gilcoto, M., J. L. Largier, E. D. Barton, S. Piedracoba, R. Torres, R. Graña, F. Alonso-Pérez, N. Villacieros-Robineau, and F. de la Granda (2017), Rapid response to coastal upwelling in a semienclosed bay, *Geophys. Res. Lett.*, *44*, 2388–2397, doi:10.1002/2016GL072416.

Received 22 DEC 2016
Accepted 17 FEB 2017
Accepted article online 21 FEB 2017
Published online 4 MAR 2017

Rapid response to coastal upwelling in a semienclosed bay

Miguel Gilcoto[1], John L. Largier[2], Eric D. Barton[1], Silvia Piedracoba[3], Ricardo Torres[4], Rocío Graña[1], Fernando Alonso-Pérez[1], Nicolás Villacieros-Robineau[5], and Francisco de la Granda[6]

[1]Instituto de Investigaciones Marinas, CSIC (IIM-CSIC), Vigo, Spain, [2]Bodega Marine Laboratory, University of California, Davis, California, USA, [3]Facultad de Ciencias del Mar, Universidad de Vigo, Vigo, Spain, [4]Plymouth Marine Laboratory, Plymouth, UK, [5]Laboratoire d'Océanographie et du Climat, Université Pierre et Marie Curie, Paris, France, [6]Bundesamt für Seeschifffahrt und Hydrographie, Hamburg, Germany

Abstract Bays/estuaries forced by local wind show bidirectional exchange flow. When forced by remote wind, they exhibit unidirectional flow adjustment to coastal sea level. Acoustic Doppler Current Profiler observations over 1 year show that the Ria de Vigo (Iberian Upwelling) responds to coastal wind events with bidirectional exchange flow. The duration of the upwelling and downwelling events, estimated from the current variability, was ~3.3 days and ~2.6 days, respectively. Vectorial correlations reveal a rapid response to upwelling/downwelling, in which currents lag local wind by $<$6 h and remote wind by $<$14 h, less than the Ekman spinup (17.8 h). This rapidity arises from the ria's narrowness (nonrotational local response), equatorward orientation (additive remote and local wind responses), depth greater than the Ekman depth (penetration of shelf circulation into the interior), and vertical stratification (shear reinforcing shelf circulation). Similar rapid responses are expected in other narrow bays where local and remote winds act together and stratification enhances bidirectional flow.

1. Introduction

The four major Eastern Boundary Upwelling Ecosystems (EBUE) of our oceans [*Fréon et al*., 2009] are among the most productive fisheries areas in the world oceans [*Pauly and Christensen*, 1995]. Coastal upwelling occurs when alongshore wind forces an offshore Ekman transport of surface water—a persistent phenomenon due to equatorward winds along midlatitude eastern boundaries of the major oceans. The divergence in Ekman transport near surface results in the upwelling of deep waters near the coast, delivering nutrients to the near-surface euphotic zone. At higher latitudes, upwelling alternates with downwelling, which occurs during poleward wind events along these eastern boundaries. The large-scale circulation in EBUE [*Hill et al*., 1998; *Mackas et al*., 2006; *Strub et al*., 2013] and the mesoscale shelf circulation [*Barth*, 2005; *Largier et al*., 2006] have been well studied, but the landward extension of coastal upwelling into bays is less well understood.

Four semienclosed and elongated bays, the Rias Baixas drowned valleys [*Evans and Prego*, 2003], are found at the northern limit of the Iberian-Canary Current EBUE (Figure 1). Coastal upwelling delivers nutrients to these rias, supporting high productivity and a major mariculture industry [*Blanton et al*., 1987]. Prior studies have shown that a residual vertical circulation in the Rías Baixas, in which upwelled water penetrates far into each ria fundamentally characterizes these bay ecosystems [*Álvarez-Salgado et al*., 2000; *Barton et al*., 2016; *Fraga*, 1981; *Souto et al*., 2003].

Bays interact with the adjacent shelf as a result of buoyancy, wind, and tidal forcing. Putting aside diffusive tidal exchanges (e.g., Tomales Bay [*Largier et al*., 1997]) and tidally induced residual circulation [*Winant*, 2008], the most effective shelf-bay exchange arises from vertical gradients in the momentum balance due to baroclinic and barotropic pressure gradients or boundary stresses. In estuaries, vertically bidirectional exchange flow with the ocean is envisaged as being purely baroclinic (induced by along-channel density gradients [*Hansen and Rattray*, 1965; *Hickey et al*., 2002]), barotropic (generated by local wind and volume conservation [*Officer*, 1976]), or a combination of both [*Blanton*, 1996]. When the remote (offshore) wind is the main barotropic forcing of the residual circulation, then the exchange flow is observed [*Noble et al*., 1996; *Walters and Gartner*, 1985; *Wang*, 1979a, 1979b; *Wong and Garvine*, 1984] and modeled numerically and analytically, as unidirectional in flat-bottomed estuaries [*Garvine*, 1985; *Janzen and Wong*, 2002; *Masse*, 1990] and as unidirectional with transverse variations in triangular, parabolic, or v-shaped cross-section estuaries [*Kasai et al*., 2000; *Valle-Levinson*, 2008; *Wong*, 1994].

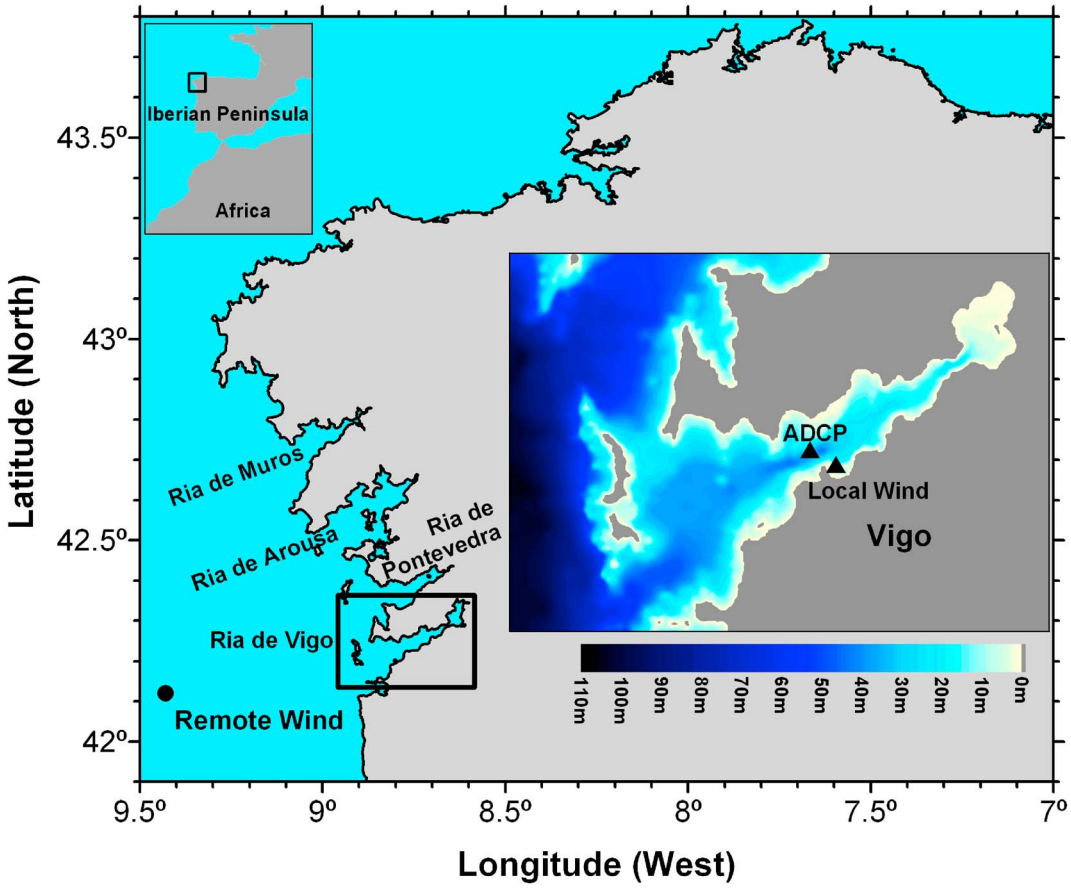

Figure 1. Map showing the four Rías Baixas of Galicia (Spain) and the locations where the remote winds (Silleiro Buoy), local winds (Vigo Harbor), and currents (ADCP in the middle of the Ría de Vigo) were recorded.

Despite the difference in vertical structure (unidirectional versus bidirectional) among remote and local wind-induced circulations, the issue of identifying which forcing is more important in a particular estuary is still a difficult task [*Wong and Mosses-Hall*, 1998; *Wong and Valle-Levinson*, 2002]. For example, equatorward facing bays seem to maintain unidirectional flows under remote upwelling winds [*Valle-Levinson et al*., 2003] and bidirectional flows with local winds [*Valle-Levinson et al*., 2004]. Interestingly, prior works in the Rias Baixas have shown that the remote wind in this coastal upwelling region interacts with the Ría de Vigo through a bidirectional exchange flow and not through a unidirectional one [*Gilcoto et al*., 2007; *Souto et al*., 2003].

In this paper, we use a yearlong record of velocity profiles in the central reaches of the Ría de Vigo to explore the bidirectional flow response to wind forcing. We find that this bidirectional exchange flow in the ria responds rapidly to the onset of winds, with lag times shorter than the inertial period which characterizes the Ekman transport response over the shelf. Our understanding is that local and remote wind forcing combine to account for this strong and rapid upwelling response, which is further enhanced by stratification associated with ria-ocean density differences. This general result can be expected in elongated bays where the two wind effects are reinforcing, but not in other elongated bays where the two effects are counteracting (e.g., Tomales Bay, California). This distinction implies that upwelling circulation (and related ecosystem productivity) will extend quickly and far into some bays in EBUE regions, but not others.

2. Data and Methods

Two meteorological stations and one Acoustic Doppler Current Profiler (ADCP) provide the data for this analysis. The meteorological stations provide 2 year time series of wind from an offshore location (remote winds) and another inside the ria (local winds), from January 2013 to December 2014. The ADCP recorded, in the center of the ria, current velocity at multiple levels for 1 year from 20 June 2013 to 13 August 2014 (Figure 1).

The offshore wind station was the Cabo Silleiro oceanographic/meteorological buoy deployed and operated by Puertos del Estado (data set available at http://www.puertos.es/en-us/oceanografia/Pages/portus.aspx). The buoy position was 9.43°W 42.12°N, on the 600 m isobath and ~70 km from the mouth of the Ría de Vigo. The recorded data, a mean over 10 min every hour, are available for 82.20% of the 2 year period. Time series of wind velocity components were screened with a 6 h filter to remove any values outside a range defined by twice the standard deviation from the window mean. Gaps shorter than 6 h were filled by linear interpolation.

In the ria, a Vantage Pro2 anemometer from Davis Instruments was installed on the breakwater of the Vigo harbor (8.757°W 42.233°N). Wind speed and direction were recorded every 1 min, and data are available for 96.77% of the 2 year measurement period. A 2 h filter (as above) was applied to remove outliers, and gaps shorter than 2 h were filled by linear interpolation. The time series was subsampled at 1 h intervals to allow direct comparison with the remote wind data.

The ADCP was deployed in the center of the channel in the middle of the ria (8.7615°W 42.2398°N), on the 45 m isobath. A 1 km submarine cable provided power and communications for real-time access to the data at a high sampling rate (2 Hz). The ADCP was a 600 kHz RDI Workhorse Sentinel with 60 levels (bins) of cell size 0.75 m. It was deployed on a ballasted pyramid with a gimbal system to level the ADCP. The currents were recorded in radial coordinates and transformed to Earth coordinates following *Gilcoto et al*. [2009]. This transformation also estimates errors for each velocity component: single-ping observations with errors greater than 20 cm/s were discarded. The 2 Hz velocities were then averaged every minute, with an estimated error of ~1.5 cm s^{-1} and subsequently subsampled hourly, yielding time series synchronous with both local and remote wind records. The ADCP also recorded water temperature at 0.6 m above the bottom (mab). ADCP observations are available for 93.76% of the 14 month deployment.

All time series were smoothed using an A24/24/25 filter [*Godin*, 1972], cutoff frequency at 67 h, to yield subtidal time series that are used in the following sections. Relationships between time series were investigated with the vector cross-correlation technique of *Kundu* [1976], which gives a determination coefficient (R^2) and the angle (α) at which maximum correlation is found. The angle of the principal axis was computed for each vector low-pass-filtered time series following *Kundu and Allen* [1976]. The significance levels of the correlations were calculated using the effective degrees of freedom, obtained by dividing the length of each series by its integral time scale estimated from the lagged autocorrelations following *Davis* [1976]. All correlation reported here are significant at the 99.0% level.

3. Results

Vertical profiles of R^2 for cross correlations between both local and remote winds and residual currents (Figure 2a) show an enhanced influence of winds near surface ($R^2 \sim 60$–70% of explained variance above 40 mab). This influence diminishes to a minimum ($R^2 \sim 5\%$) at ~33 mab but increases again with depth until ~25 mab where it remains more or less constant ($R^2 \sim 50$–60%) until the bottom. This correlation profile clearly demarcates a surface layer (>36 mab) and a bottom layer (<30 mab), where the wind explains more than 50% of the variance of the residual current, separated by a thin transition layer.

Similarly, the two-layer structure is evident in the profiles of α for both winds (Figure 2b). Near-surface currents are best correlated in the direction of the local wind forcing ($\alpha \sim 2.3°$), while near-bottom currents are best correlated in a direction almost opposed to the wind ($\alpha \sim 171.3°$). For remote winds, the angle of maximum correlation for surface currents in the ria is ~326.4° (i.e., when winds over the shelf are northward, near-surface currents in the ria flow in a direction 35.6° east of north—into the ria), while near-bottom currents have maximum correlation at $\alpha \sim 137.2°$ (i.e., flow out of the ria during northward winds offshore).

These directional relationships between winds and currents are illustrated in Figure 3, with the wind direction shown as the principal axes for the 2 year time series. The principal axis for remote winds is oriented approximately north-south (13° east of north), while the local wind is oriented more east-west, parallel to the axis of the ria (72° east of North). Importantly, in both cases (local and remote) the α values are such that the currents are also oriented along the axis of the ria. Near-surface waters move out of the ria during southward winds over the shelf and westward winds over the ria, while near-bottom waters move landward (i.e., upwelling vertical circulation; Figures 3c and 3d). In contrast, during northward winds over the shelf and eastward

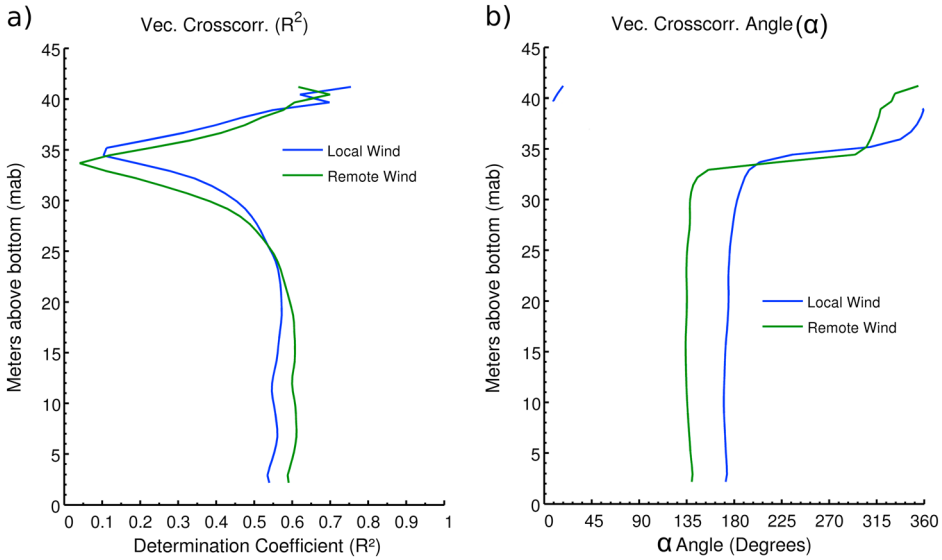

Figure 2. Vertical profiles of (a) determination coefficient (R^2) and (b) direction of best correlation (counterclockwise from currents) corresponding to vectorial cross correlations between filtered-wind and residual-current time series.

winds over the ria, near-surface waters move into the ria, while near-bottom waters move seaward (i.e., downwelling vertical circulation; Figures 3e and 3f).

Winds both offshore and over the ria are related to large-scale atmospheric patterns and can be expected to be correlated. Vector correlation between wind records gives $R^2 \sim 80\%$ with maximum correlation found at an angle of $\alpha \sim 26°$, so that southward winds over the shelf are strongly correlated with southwestward winds over the ria (and northeastward winds over the ria correlate with northward winds over the shelf). However, winds over the ria tend to lag winds over the shelf by a few hours: maximum correlation is at 3 h (Figure 4a), but the lagged correlation curve has a broad peak because it includes variation over a whole year. In individual events, the ria winds can lag shelf winds by half a day or even lead shelf winds by few hours, depending on the speed and propagation direction of synoptic meteorological features.

Also important is the lag in the response of currents to winds (Figures 4c and 4d). Currents in the ria respond immediately and uniformly to local winds (lag less than 1 h), except in the interface layer where R^2 is lower. For forcing by remote winds, the response time increases to 6–8 h, with more variable lags through the water column. However, while these lags represent maximum correlations, the correlation peaks are not sharp as the fluctuations in low-pass-filtered winds and currents have time scales longer than a day (Figure 4d).

To examine the more event-driven nature of the ria subtidal dynamics, a running window technique was applied to the time series. The lagged Kundu vectorial cross correlations between wind and residual currents in the surface and bottom layers were estimated in windows of 9 and 6 days for remote and local winds, respectively, long enough to frame inside them a complete upwelling or downwelling long event while short enough to include only one or two short events. The lag of maximum R^2 was obtained for each window across the complete 1 year record (Figures 4e and 4f). For both winds and in both layers, the most frequent lag class is that shorter than 1 h related to events that persist longer than the window length. For the local wind, the most probable lag is 4 h and then longer lags are less common. In contrast, the remote wind shows high relative frequency values at lags around 12 ± 1 and 10 ± 1 h for the bottom and surface layers, respectively.

4. Discussion

Prior studies in the Rias Baixas have identified remote wind as the primary forcing of residual circulation in these rias [*Álvarez-Salgado et al.*, 2000; *Fraga*, 1981; *Pardo et al.*, 2001; *Rosón et al.*, 1997]. Although in the external part of the Ria de Vigo a three-dimensional circulation may take place [*Barton et al.*, 2015; *Gilcoto et al.*, 2007; *Piedracoba et al.*, 2016; *Souto et al.*, 2003], in the middle ria the classical bidirectional exchange

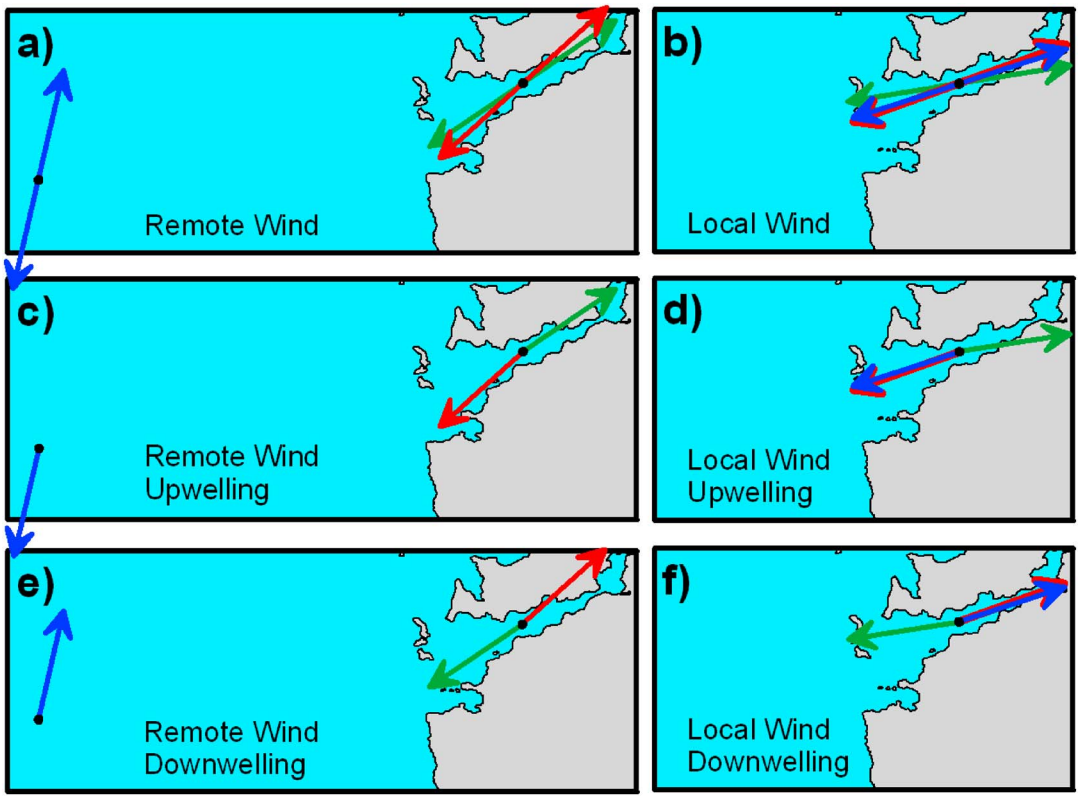

Figure 3. Plan view of the geometric relationships between wind and current patterns—depicted with arrows overlaid on a map of the Ría de Vigo. Blue arrows correspond to the principal axes of winds (remote on the left column and local on the right) while the red and green arrows to the directions of the surface (>36 mab) and bottom (<30 mab) layers, respectively, of the residual currents rotated following maximum correlation angles between currents and winds (see text). (a, b) The general case, with both senses for each arrow direction. The arrows (c, d) for upwelling conditions and (e, f) for downwelling.

flow sketched in Figure 11 of *Villacieros-Robineau et al*. [2013] is seen clearly in our vector cross correlations. Based on these correlations between long data series, our results reaffirm the importance of remote winds—they explain more variance in residual currents than the local wind—although the two wind signals are well correlated with each other (Figure 4a), which makes the identification of the main forcing difficult. The high- and low-pressure systems in this region usually travel from the Atlantic Ocean toward Europe (west to east) with spatial scales of hundreds of kilometers, larger than the length of the ria (~30 km). The distance between the local and remote wind stations is 82 km, while the wind signal propagates between them in ~3 h (Figure 4a), a sensible traveling velocity (~27 km/h) for a storm (high-pressure system) generating intense downwelling (upwelling).

Based on wind data, both *Nogueira et al*. [1997] and *Torres et al*. [2003] estimated that the average duration of a complete upwelling/downwelling cycle is 14–15 days. However, *Nogueira et al*. [1997] also showed that the seasonal cycle of the Ekman transport over the shelf accounts for only ~20% of the total variance, with additional variance due to higher frequencies. Instead of using wind observations, we can now directly observe the number and duration of upwelling and downwelling events with the filtered ADCP time series (Figure 4b). The most common of upwelling events is only 1 day long and the average length is ~3.3 days; the most common of downwelling events is 2 days long and the average length is ~2.6 days. Therefore, despite the tail in the histogram of event durations, the ADCP indicates event lengths notably shorter than the 7–8 day length implied by earlier analyses of wind data.

Not only are upwelling events shorter than thought. The year-round average response, estimated as the lag for maximum correlation, is only 8 h for remote wind and <1 h for local wind. Several authors have already noted that the residual circulation in the ria can respond rapidly to wind events [*Piedracoba et al*., 2005; *Souto et al*., 2003; *Villacieros-Robineau et al*., 2013]. However, the Ekman response in cross-shelf currents is expected to occur on a time scale given by the inertial period (17.8 h). To account for the transient and

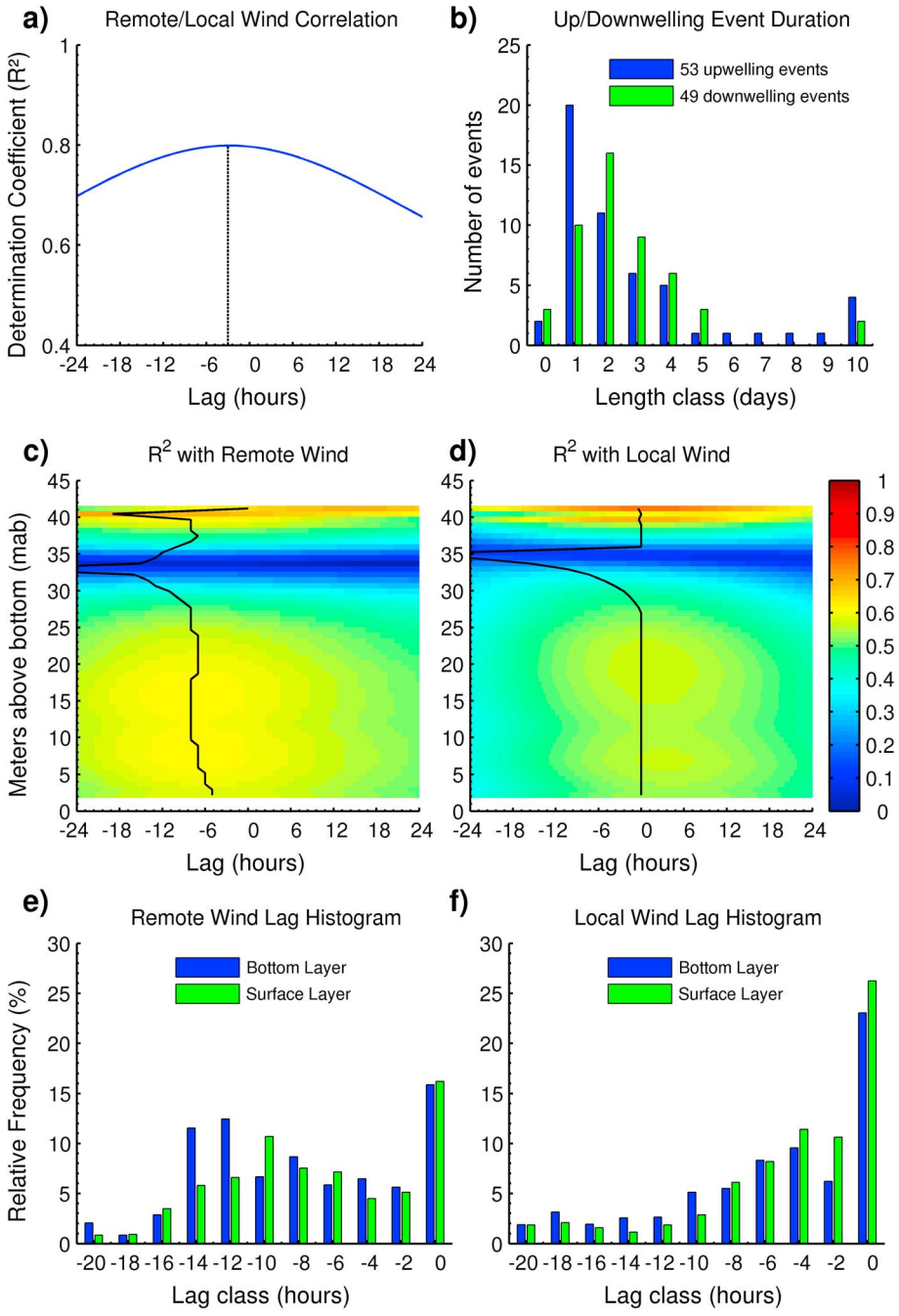

Figure 4. (a) Lagged vectorial cross correlation between remote and local winds; negative lag if remote leads local wind. (b) Histogram showing duration of upwelling (blue) and downwelling (green) events determined by periods of bidirectional flow observed in the ADCP record. Every period of time longer than 8 h is considered "upwelling" if the residual current in the surface layer (37–42 mab) was >5 cm s^{-1} outward and simultaneously >5 cm s^{-1} inward in the bottom layer (16–26 mab). And "downwelling" when current was inward in surface layer and outward in bottom layer. (c) Contour plots with determination coefficients (R^2) from vectorial cross correlations between filtered remote winds and residual currents as a function of depth (mab) and lag (hours); negative lags indicate that the wind leads the current. The black line joins the lags of maximum R^2 for each depth. (d) Same for local winds. (e) Histograms represent the relative frequency of 9 day wind current lags of maximum vectorial cross correlation between residual currents, in the surface layer (blue bars) and bottom layer (green bars), with remote winds. (f) Same for local winds, but with 6 day window.

event-driven nature of the residual circulation of the ria, lagged vectorial cross correlations were calculated between wind and current in running windows of 6 (local wind) or 9 (remote wind) days. In this way, it was found that the event response time of the surface and bottom layer to remote wind increases to 10 and 12 h, respectively (Figure 4e). These lag times are closer to the inertial period but still 22% shorter. Slower responses are observed in bays topographically sheltered [*Rosenfeld et al*., 1994] or when responses are due to classical gravitational circulation [*Hansen and Rattray*, 1965], to shelf-bay density differences [*Blanton*, 1996; *Hickey et al*., 2002; *Monteiro and Largier*, 1999], to the interaction of the alongshore coastal jet with topography [*Graham and Largier*, 1997; *Ryan et al*., 2009], and to a headland eddy (e.g., St. Helena Bay [*Penven et al*., 2000]). Therefore, we suggest that the initial forcing of bidirectional circulation in the ria is local wind stress.

The purely barotropic effect of local wind stress on residual currents in estuaries [*Officer*, 1976], in lakes [*Csanady*, 1973], and over the inner shelf [*Lentz and Fewings*, 2012] has been shown to be bidirectional, with a surface layer driven directly by wind stress and a bottom layer driven by a pressure gradient due to the slope in the sea surface setup. In contrast, remote winds are expected to induce a unidirectional flow [*Garvine*, 1985; *Wong*, 1994]. As the remote wind blows on the shelf, it produces a large-scale (compared with the estuary length) sea level setup or setdown at the mouth of the estuary and a net unidirectional inflow or outflow. Nevertheless, if the depth of the estuary mouth is deeper than the Ekman depth then, instead of the unidirectional flow due to sea level variations, the standard two-layer upwelling/downwelling circulation can also penetrate into the estuary [*Gilcoto et al*., 2007; *Souto et al*., 2003].

The response to wind stress over the shelf is expected to develop slowly over an inertial period when starting smoothly from a calm situation. However, the bidirectional exchange flow in the ria develops quickly as the weather fronts, large compared with the ria dimensions, approach the coast since the local wind stress on the ria associated with arrival of the weather front can be expected to drive a rapid response in the surface layer of the ria and establish a bidirectional flow within a few hours (Figures 4d and 4f). This bidirectional flow in the ria due to local easterlies (westerlies) is accompanied by upwelling (downwelling) favorable winds over the shelf, which spin-up Ekman transport and coastal upwelling within an inertial period. Thus, the transport due to nonrotational wind-driven surface flow in the ria merges with the developing rotational (Ekman) wind-driven surface flow over the shelf and takes control of the residual circulation of the ria. In this way, the Ekman response over the shelf extends rapidly far into the ria in a way previously not observed in upwelling bays [*Valle-Levinson et al*., 2003; *Valle-Levinson et al*., 2004] but which may resemble the important effects of coastal upwelling on fjords [*Erga et al*., 2012; *Straneo et al*., 2010].

In spite of the secondary role of buoyancy forcing in longitudinal exchange flow in the ria, stratification plays an important role in its response to upwelling winds. In the first few days, westward winds over the ria advect warm low-salinity water from the inner ria over denser outer ria waters and later the upwelling of cold dense water at the mouth of the ria and intrusion in the bottom layer maintains stratification [*Barton et al*., 2015; *Gilcoto et al*., 2007]. Stratification retains the momentum gain from surface wind stress in a well-defined, shallow surface layer, allowing rapid acceleration and strong shear across the pycnocline. This stratification also allows the deeper waters to simultaneously move in the opposite direction with minimal fluid drag. Stratification may not be maintained during downwelling events, the shear in the bidirectional flow may weaken, although it will persist as long as wind forcing persists [*Barton et al*., 2016]. Sometimes a buoyant surface layer may also form during downwelling phases, when low-salinity waters in the Western Iberian Buoyancy Current [*Peliz et al*., 2005] are found at the mouth of the ria [*Mouriño and Fraga*, 1982].

This study of a long, narrow bay in the Galician upwelling region provides insight useful for understanding bays more generally in upwelling regions. Three factors account for the rapid extension of upwelling far into this ria bay—in other bays upwelling may not extend as far or not as quickly. First, the bay is narrower than the Rossby radius so that the primary response to local winds is nonrotational and rapid. Second, its orientation ensures that local winds inside the bay drive transport in the surface boundary layer in the same direction as the Ekman layer transport over the shelf; the opposite occurs in bays that face into upwelling winds, e.g., Tomales Bay, California. Third, vertical stratification supports strong and shallow vertical shear that allows a more rapid response and extension of the vertical circulation further into the bay. Thus, the aspect ratio of the ria (length $\gg$ width) has allowed us to address two associated but distinct roles of surface wind stress in upwelling bays—both the remote wind stress over the shelf and local wind stress over the ria. In many

smaller bays, the size/shape of the bay [*Monteiro and Largier*, 1999] or the complexity of the wind field [*Paduan and Rosenfeld*, 1996] precludes a clear exposition of these two forcing mechanisms. Also, we differentiate the two roles of density structure: (i) longitudinal density gradients that may drive an estuarine circulation and (ii) vertical density gradients that enable high vertical shear.

This description of vertical circulation in the Ria de Vigo shows the importance of specific bay characteristics that allow extension of the shelf upwelling system far into the sheltered waters of the bay. This helps to explain the extent and reliability of the productive ecosystem and high levels of bivalve culture in the ria [*Figueiras et al*., 2002], which is not found in all upwelling bays. Given the high frequency of upwelling/downwelling wind variability in this region [*Nogueira et al*., 1997], the rapid response of the ria means that the basin is well flushed, ensuring a continuous influx of high-nutrient waters and removal of any oxygen depletion effects in the ria. In comparable but shallower bays, or bays with local winds opposed to wind effects over the shelf, like Tomales Bay, this rapid exchange does not happen and the midbay/inner bay exhibits severe nutrient depletion and reduced productivity [*Kimbro et al*., 2009].

5. Conclusions

Vectorial cross correlations, between winds measured at two different locations (remote and local) and water velocity profiles recorded in the interior of the Ria de Vigo allowed us to examine the forcing of the bidirectional flow in the residual circulation of the ria. Both determination coefficients and angles of maximum correlation portrayed this vertical structure. Residual currents are more correlated with remote than with local winds. Both winds are also well correlated with each other since they are driven by the incoming eastward traveling atmospheric lows and highs.

The response of the residual currents in the ria to the winds is fast. Local wind produces responses within 6 h, while the lag associated with remote wind is twice as long. Even the latter is faster than the spin-up time (~17.8 h) of the coastal upwelling. Further, the average duration of upwelling events is ~3.3 days and of downwelling events is ~2.6 days. Therefore, ria subtidal dynamics, revealed by direct current observations, are more rapid and variable in time than suggested by previous estimations from winds.

The rapid response of the ria to the wind encourages us to consider the wind-driven barotropic bidirectional flow as the first-order mechanism of residual circulation in the ria. In such mechanism, the upwelling/downwelling cross-shelf circulation structure penetrates into the ria aided by an internal bidirectional flow initiated by local wind and the reduction of friction between layers generated by preexisting vertical stratification. More studies must be undertaken to increase our knowledge on secondary forcings that may modulate the residual circulation of the Rias Baixas, or primary forcings that predominate in other types of events.

Acknowledgments
Thanks are due to UMT-CSIC technicians, the captains, and crews of B/O *Mytilus* (CSIC) and *Berbes* boats (Vigo Port Authority). The field work and data analysis were supported by the Spanish Ministry of Economy and Competitivity under STRAMIX research project (CTM2012-35155). Writing up was completed with the aid of support from Xunta de Galicia (Contrato Programa Xunta-CSIC). J.L.L. thanks California Sea grant (2014-R/HCME-04) for support. The data used are listed in section 2, ADCP data can be downloaded from http://soco.iim.csic.es. We also acknowledge useful comments of two anonymous reviewers.

References

Álvarez-Salgado, X. A., J. Gago, B. M. Míguez, M. Gilcoto, and F. F. Pérez (2000), Surface waters of the NW Iberian margin: Upwelling on the shelf versus outwelling of upwelled waters from the Rías Baixas, *Estuarine Coastal Shelf Sci.*, *51*(6), 821–837.

Barth, J. A. (2005), Introduction to special section: Coastal advances in shelf transport, *J. Geophys. Res.*, *110*, C10S01, doi:10.1029/2005JC003124.

Barton, E. D., J. L. Largier, R. Torres, M. Sheridan, A. Trasviña, A. Souza, Y. Pazos, and A. Valle-Levinson (2015), Coastal upwelling and downwelling forcing of circulation in a semi-enclosed bay: Ria de Vigo, *Prog. Oceanogr.*, *134*, 173–189.

Barton, E. D., R. Torres, F. G. Figueiras, M. Gilcoto, and J. Largier (2016), Surface water subduction during a downwelling event in a semienclosed bay, *J. Geophys. Res. Oceans*, *121*, 7088–7107, doi:10.1002/2016JC011950.

Blanton, J. O. (1996), Reinforcement of gravitational circulation by wind, in *Buoyancy Effects on Coastal and Estuarine Dynamics*, edited by D. G. Aubrey and C. T. Friedrichs, pp. 47–58, AGU, Washington, D. C.

Blanton, J. O., K. R. Tenore, F. Castillejo, L. P. Atkinson, F. B. Schwing, and A. Lavín (1987), The relationship of upwelling to mussel production in the rias on the western coast of Spain, *J. Mar. Res.*, *45*(2), 497–511.

Csanady, G. T. (1973), Wind-induced barotropic motions in long lakes, *J. Phys. Oceanogr.*, *3*(4), 429–438.

Davis, R. E. (1976), Predictability of sea surface temperature and sea level pressure anomalies over the North Pacific Ocean, *J. Phys. Oceanogr.*, *6*(3), 249–266.

Erga, S. R., N. Ssebiyonga, Ø. Frette, B. Hamre, J. Aure, Ø. Strand, and T. Strohmeier (2012), Dynamics of phytoplankton distribution and photosynthetic capacity in a western Norwegian fjord during coastal upwelling: Effects on optical properties, *Estuarine Coastal Shelf Sci.*, *97*, 91–103.

Evans, G., and R. Prego (2003), Rias, estuaries and incised valleys: Is a ria an estuary?, *Mar. Geol.*, *196*(3–4), 171–175.

Figueiras, F. G., U. Labarta, and M. J. Reiriz (2002), Coastal upwelling, primary production and mussel growth in the Rías Baixas of Galica, *Hydrobilogia*, *484*, 121–131.

Fraga, F. (1981), Upwelling off the Galician coast, northwest Spain, in *Coastal Upwelling*, *Coastal and Esturarine Sci.*, vol. 1, edited by F. A. Richards, pp. 176–182, AGU, Washington, D. C.

Fréon, P., M. Barange, and J. Arístegui (2009), Eastern boundary upwelling ecosystems: Integrative and comparative approaches, *Prog. Oceanogr.*, *83*(1–4), 1–14.
Garvine, R. W. (1985), A simple model of estuarine subtidal fluctations forced by local and remote wind stress, *J. Geophys. Res.*, *90*, 11,945–11,948, doi:10.1029/JC090iC06p11945.
Gilcoto, M., P. C. Pardo, X. A. Álvarez-Salgado, and F. F. Pérez (2007), Exchange fluxes between the Ría de Vigo and the shelf: A bidirectional flow forced by remote wind, *J. Geophys. Res.*, *112*, C06001, doi:10.1029/2005JC003140.
Gilcoto, M., E. Jones, and L. Fariña-Busto (2009), Robust estimations of current velocities with four-beam broadband ADCPs, *J. Atmos. Oceanic Technol.*, *26*(12), 2642–2654.
Godin, G. (1972), *The Analysis of Tides*, pp. 264, Liverpool Univ. Press, Liverpool.
Graham, W. M., and J. L. Largier (1997), Upwelling shadows as nearshore retention sites: The example of northern Monterey Bay, *Cont. Shelf Res.*, *17*(5), 509–532.
Hansen, D. V., and M. Rattray (1965), Gravitational circulation in straits and estuaries, *J. Mar. Res.*, *23*(2), 104–122.
Hickey, B. M., X. Zhang, and N. Banas (2002), Coupling between the California Current System and a coastal plain estuary in low riverflow conditions, *J. Geophys. Res.*, *107*(C10), 3166, doi:10.1029/1999JC000160.
1Hill, A. E., B. M. Hickey, F. A. Shillington, P. T. Strub, K. H. Brink, E. D. Barton, and A. C. Thomas (1998), Eastern ocean boundaries, in *The Global Coastal Ocean: Regional Studies and Syntheses*, edited by A. R. Robinson and K. H. Brink, pp. 29–67, Harvard Univ. Press, Cambridge.
Janzen, C. D., and K.-C. Wong (2002), Wind-forced dynamics at the estuary-shelf interface of a large coastal plain estuary, *J. Geophys. Res.*, *107*(C10), 3138, doi:10.1029/2001JC000959.
Kasai, A., A. E. Hill, T. Fujiwaka, and J. H. Simpson (2000), Effect of the Earth's rotation on the circulation in regions of freshwater influence, *J. Geophys. Res.*, *105*, 16,961–16,969, doi:10.1029/2000JC900058.
Kimbro, D. L., J. L. Largier, and E. D. Grosholz (2009), Coastal oceanographic processes influence the growth and size of a key estuarine species, the Olympia oyster, *Limnol. Oceanogr.*, *54*(5), 1425–1437.
Kundu, P. K. (1976), Ekman veering observed near the ocean bottom, *J. Phys. Oceanogr.*, *6*(2), 238–242.
Kundu, P. K., and J. S. Allen (1976), Some three-dimensional characteristics of low-frequency current fluctuations near the Oregon coast, *J. Phys. Oceanogr.*, *6*(2), 181–199.
Largier, J. L., J. T. Hollibaugh, and S. V. Smith (1997), Seasonally hypersaline estuaries in Mediterranean-climate regions, *Estuarine Coastal Shelf Sci.*, *45*(6), 789–797.
Largier, J. L., et al. (2006), WEST: A northern California study of the role of wind-driven transport in the productivity of coastal plankton communities, *Deep Sea Res., Part II*, *53*(25–26), 2833–2849.
Lentz, S. J., and M. R. Fewings (2012), The wind- and wave-driven inner-shelf circulation, *Annu. Rev. Mar. Sci.*, *4*, 317–343.
Mackas, D. L., P. T. Strub, A. Thomas, and V. Montecino (2006), Eastern regional ocean boundaries pan-regional overview, in *The Global Coastal Ocean, Interdisciplinary Regional Studies and Syntheses. Panregional Syntheses and the Coast of North and South America and Asia*, edited by A. R. Robinson and K. H. Brink, pp. 21–59, Harvard Univ. Press, Cambridge.
Masse, A. K. (1990), Withdrawal of shelf water into an estuary: A barotropic model, *J. Geophys. Res.*, *95*, 16,085–16,096, doi:10.1029/JC095iC09p16085.
Monteiro, P. M. S., and J. L. Largier (1999), Thermal stratification in Saldanha Bay (South Africa) and subtidal, density-driven exchange with the coastal waters of the Benguela Upwelling System, *Estuarine Coastal Shelf Sci.*, *49*(6), 877–890.
Mouriño, C., and F. Fraga (1982), Hidrografía de la Ría de Vigo. 1976–1977. Influencia anormal del Río Miño, *Invest. Pesq.*, *46*(3), 459–468.
Noble, M. A., W. W. Schoeder, W. J. Wiseman Jr., H. F. Ryan, and G. Gelfenbaum (1996), Subtidal circulation patterns in a shallow, highly stratified estuary: Mobile Bay, Alabama, *J. Geophys. Res.*, *101*, 25,689–25,703, doi:10.1029/96JC02506.
Nogueira, E., F. F. Pérez, and A. F. Ríos (1997), Seasonal patterns and long-term trends in an estuarine upwelling ecosystem (Ría de Vigo, NW Spain), *Estuarine Coastal Shelf Sci.*, *44*(3), 285–300.
Officer, C. B. (1976), *Physical Oceanography of Estuaries (and Associted Coastal Waters)*, pp. 465, John Wiley, New York.
Paduan, J. D., and L. K. Rosenfeld (1996), Remotely sensed surface currents in Monterey Bay from shore-based HF radar (Coastal Ocean Dynamics Application Radar), *J. Geophys. Res.*, *101*, 20,669–20,686, doi:10.1029/96JC01663.
Pardo, P. C., M. Gilcoto, and F. F. Pérez (2001), Short-time scale coupling between termohaline and meteorological forcing in the Ría de Pontevedra, *Sci. Marina*, *65*(S1), 229–240.
Pauly, D., and V. Christensen (1995), Primary production required to sustain global fisheries, *Nature*, *374*, 255–257.
Peliz, Á., J. Dubert, A. M. P. Santos, P. B. Oliveira, and B. Le Cann (2005), Winter upper ocean circulation in the Western Iberian Basin—Fronts, eddies and poleward flows: An overview, *Deep Sea Res., Part I*, *52*(4), 621–646.
Penven, P., C. Roy, A. Colin de Verdière, and J. Largier (2000), Simulation of a coastal jet retention process using a barotropic model, *Oceanol. Acta*, *23*(5), 615–634.
Piedracoba, S., X. A. Álvarez-Salgado, G. Rosón, and J. L. Herrera (2005), Short-timescale thermohaline variability and residual circulation in the central segment of the coastal upwelling system of the Ría de Vigo (northwest Spain) during four contrasting periods, *J. Geophys. Res.*, *110*, C03018, doi:10.1029/2004JC002556.
Piedracoba, S., G. Rosón, and R. A. Varela (2016), Origin and development of recurrent dipolar vorticity structures in the outer Ría de Vigo (NW Spain), *Cont. Shelf Res.*, *118*, 143–153.
Rosenfeld, L. K., F. B. Schwing, N. Garfield, and D. E. Tracy (1994), Bifurcated flow from an upwelling center: A cold water source for Monterey Bay, *Cont. Shelf Res.*, *14*(9), 931–964.
Rosón, G., X. A. Álvarez-Salgado, and F. F. Pérez (1997), A non-stationary box model to determine residual fluxes in a partially mixed estuary, based on both thermohaline properties: Application to the Ria de Arousa (NW Spain), *Estuarine Coastal Shelf Sci.*, *44*(3), 249–262.
Ryan, J. P., A. M. Fischer, R. M. Kudela, J. F. R. Gower, S. A. King, R. Marin, and F. P. Chavez (2009), Influences of upwelling and downwelling winds on red tide bloom dynamics in Monterey Bay, California, *Cont. Shelf Res.*, *29*(5–6), 785–795.
Souto, C., M. Gilcoto, L. Fariña-Busto, and F. F. Pérez (2003), Modelling the residual circulation of a coastal embayment affected by wind driven upwelling: Circulation of the Ria de Vigo (NW Spain), *J. Geophys. Res.*, *108*(C11), 3340, doi:10.1029/2002JC001512.
Straneo, F., G. S. Hamilton, D. A. Sutherland, L. A. Stearns, F. Davidson, M. O. Hammill, G. B. Stenson, and A. Rosing-Asvid (2010), Rapid circulation of warm subtropical waters in a major fjord in East Greenland, *Nat. Geosci.*, *3*(3), 182–186.
Strub, P. T., V. Combes, F. A. Shillington, and O. Pizarro (2013), Currents and processes along the eastern boundaries, in *Ocean Circulation and Climate. A 21st Century Perspective*, edited by G. Siedler et al., pp. 339–384, Elsevier-Academic Press, Amsterdam.
Torres, R., E. D. Barton, P. Miller, and E. Fanjul (2003), Spatial patterns of wind and sea surface temperature in the Galician upwelling region, *J. Geophys. Res.*, *108*(C4), 3130, doi:10.1029/2002JC001361.

Valle-Levinson, A. (2008), Density-driven exchange flow in terms of the Kelvin and Ekman numbers, *J. Geophys. Res.*, *113*, C04001, doi:10.1029/2007JC004144.
Valle-Levinson, A., L. P. Atkinson, D. Figueroa, and L. Castro (2003), Flow induced by upwelling winds in an equatorward facing bay: Gulf of Arauco, Chile, *J. Geophys. Res.*, *108*(C2), 3054, doi:10.1029/2001JC001272.
Valle-Levinson, A., et al. (2004), Wind-induced exchange at the entrance to Concepción Bay, an equatorward facing embayment in central Chile, *Deep Sea Res., Part II*, *51*(20–21), 2371–2388.
Villacieros-Robineau, N., J. L. Herrera, C. G. Castro, S. Piedracoba, and G. Roson (2013), Hydrodynamic characterization of the bottom boundary layer in a coastal upwelling system (Ría de Vigo, NW Spain), *Cont. Shelf Res.*, *68*, 67–79.
Walters, R. A., and J. W. Gartner (1985), Subtidal sea level and current variations in the Northern Reach of San Francisco Bay, *Estuarine Coastal Shelf Sci.*, *21*, 17–32.
Wang, D.-P. (1979a), Wind-driven circulation in the Chesapeak Bay, winter 1975, *J. Phys. Oceanogr.*, *9*, 564–572.
Wang, D.-P. (1979b), Subtidal sea level variations in the Chesapeake Bay and relations to atmospheric forcing, *J. Phys. Oceanogr.*, *9*, 413–421.
Winant, C. D. (2008), Three-dimensional residual tidal circulation in an elongated, rotating basin, *J. Phys. Oceanogr.*, *38*(6), 1278–1295.
Wong, K.-C. (1994), On the nature of transverse variability in a coastal plain estuary, *J. Geophys. Res.*, *99*, 14,209–14,222, doi:10.1029/94JC00861.
Wong, K.-C., and A. Valle-Levinson (2002), On the relative importance of the remote and local wind effects on the subtidal exchange at the entrance to the Chesapeake Bay, *J. Mar. Res.*, *60*(3), 477–498.
Wong, K.-C., and J. E. Mosses-Hall (1998), On the relative importance of the remote and local wind effects to the subtidal variability in a coastal plain estuary, *J. Geophys. Res.*, *103*, 18,393–18,404, doi:10.1029/98JC01476.
Wong, K.-C., and R. W. Garvine (1984), Observations of wind-induced, subtidal variability in the Delaware Estuary, *J. Geophys. Res.*, *89*, 10,589–10,597, doi:10.1029/JC089iC06p10589.